Title

IL-1 beta and TNF-alpha upregulate angiotensin II type 1 (AT(1)) receptors on cardiac fibroblasts and are associated with increased AT(1) density in the post-MI heart

Journal

Journal of Molecular and Cellular Cardiology, 38(3)

ISSN

0022-2828

Authors

Gurantz, D
Cowling, R T
Varki, N
et al.

Publication Date

2005-03-01

Peer reviewed

ARTICLE IN PRESS

Available online at www.sciencedirect.com

SCIENCE DIRECT®

Journal of Molecular and Cellular Cardiology ■■ (2005) ■■■-■■■

Journal of Molecular and Cellular Cardiology

www.elsevier.com/locate/yjmcc

Original article

IL-1β and TNF-α upregulate angiotensin II type 1 (AT_1) receptors on cardiac fibroblasts and are associated with increased AT_1 density in the post-MI heart

Devorah Gurantz [a], Randy T. Cowling [a], Nissi Varki [b], Eduardo Frikovsky [a], Cristina D. Moore [a], Barry H. Greenberg [a,*]

[a] *Division of Cardiology, Department of Medicine, University of California, San Diego Medical Center, 200 W Arbor Drive, San Diego, CA 92103-8411, USA*

[b] *Departments of Pathology and Medicine, University of California, San Diego Medical Center, San Diego, CA 92103-8411, USA*

Received 4 August 2004; received in revised form 15 December 2004; accepted 30 December 2004

Abstract

Angiotensin (Ang) II plays an important role in post-myocardial infarction (MI) cardiac remodeling. The Ang II type 1 (AT_1) receptor which mediates most Ang II effects is upregulated on non-myocytes in the post-MI heart. We have shown that pro-inflammatory cytokines increase AT_1 receptor density on cardiac fibroblasts through a mechanism involving NF-κB activation. This study examines the in vitro kinetics of tumor necrosis factor-α (TNF-α) and interleukin-1β (IL-1β) induced AT_1 receptor upregulation in neonatal rat cardiac fibroblasts and assesses temporal and spatial associations between the appearance of these agents and increased AT_1 receptor density post-MI. The results show that IL-1β more rapidly induces AT_1 receptor upregulation than does TNF-α, an effect that can be mimicked by a NF-κB-dependent luciferase reporter gene. Moreover, the effects of these pro-inflammatory cytokines are additive. Using immunohistochemistry in the post-MI rat heart we found strong temporal and spatial correlations between TNF-α, IL-1β and AT_1 receptor proteins in the peri-infarction (PI) zone in fibroblasts and macrophages. Labeling intensity for the cytokines and the AT_1 receptor increased from 1 to 7 days post-MI in the PI zone in conjunction with replacement scar formation. This labeling persisted in non-myocytes bordering the scar for up to 83 days post-MI. These findings suggest that IL-1β and TNF-α act coordinately to increase AT_1 receptor density on non-myocytes in the post-MI heart and that this effect may contribute to extracellular matrix remodeling and fibrosis.

Keywords: AT_1 receptor; Cardiac fibroblast; Tumor necrosis factor-α (TNF-α); Interleukin-1β (IL-1β); Post-myocardial infarction remodeling

1. Introduction

Post-myocardial infarction (MI) the heart undergoes a process of remodeling that includes both hypertrophy of cardiac myocytes in non-infarcted segments of myocardium and extensive changes in the extracellular matrix (ECM). The latter involves formation of a replacement scar at the infarct site as well as deposition of fibrous tissue throughout the remaining spared segments of myocardium. Changes that occur in the ECM in the post-MI heart are important determinants of cardiac function. The expeditious generation of a replacement scar helps maintain structural integrity of the heart and limits further increases in chamber size that would increase wall stress and load on the damaged ventricle. Fibrous tissue deposition in non-infarcted myocardium, however, adversely affects cardiac function and is a major factor in the development of heart failure [1].

Cardiac fibroblasts are critical components in the post-MI ECM remodeling process [2]. Angiotensin (Ang) II stimulates fibroblast functions that are involved in ECM remodeling including the production of structural ECM proteins such as fibronectin and collagens (Col) I and III, tissue inhibitors of matrix metalloproteinases (TIMPs) and 'secondary' growth factors that act in an autocrine/paracrine manner to promote the remodeling process [3–7]. The Ang II type 1 (AT_1) receptor mediates most of these Ang II effects and there is evi-

* Corresponding author. Tel.: +1-619-543-7751; fax: +1-619-543-7870.
E-mail address: bgreenberg@ucsd.edu (B.H. Greenberg).

0022-2828/$ - see front matter © 2005 Published by Elsevier Ltd.
doi:10.1016/j.yjmcc.2004.12.015

dence that AT_1 density is upregulated on cardiac fibroblasts in the post-MI heart [8,9]. Moreover, the administration of Ang converting enzyme (ACE) inhibitors and Ang receptor blockers inhibits post-MI fibrosis in animal models [10–15] and improves the clinical course in these experimental settings as well as in post-MI patients [16,17].

We have previously shown that tumor necrosis factor-α (TNF-α) and interleukin-1β (IL-1β), pro-inflammatory cytokines that are present in the post-MI heart [18–21], upregulate the AT_1 receptor in cultured rat neonatal cardiac fibroblasts [22] through a mechanism involving NF-κB activation [23]. This effect appears to be important since cytokine induced increases in AT_1 receptor density enhance the response to Ang II of fibroblast functions that favor ECM deposition [24]. These findings raise the possibility that TNF-α and IL-1β coordinately regulate AT_1 receptor density on cardiac fibroblasts within the post-MI heart. While such cooperation might provide both greater precision and increased options for controlling AT_1 receptor expression, redundancy in the effects of these cytokines also suggests that interventions which inhibit individual cytokines might not be optimal, at least in regard to the regulation of the AT_1 receptor. Thus, this study was designed to: 1) characterize and compare the time- and dose-dependent effects of IL-1β and TNF-α on AT_1 receptor expression in cardiac fibroblasts, 2) correlate the timing of cytokine induced NF-κB activation with AT_1 gene expression, and 3) determine spatial and temporal associations between the appearance of IL-1β and TNF-α and AT_1 upregulation in the post-MI heart and the appearance of these proteins with the deposition of fibrous tissue at the infarct site.

2. Materials and methods

2.1. Cell cultures

Neonatal rat cardiac fibroblasts were prepared from hearts of 1–2 day-old Sprague–Dawley rats as described [6]. For each experiment fibroblasts were plated from frozen stock (passage 1) in media (DMEM high glucose; Gibco-BRL, Gaithersburg, MD) containing 10% FBS. At 100% confluence media was replaced with serum-free media for 24 h and cultures were treated according to the experimental design. Three independent experiments were done using three different cell preparations. In time course experiments fibroblasts from the same culture were exposed to recombinant rat IL-1β (1 ng/ml, R&D Systems) or recombinant rat TNF-α (10 ng/ml, Biosource International, Camarillo, CA) in serum-free media for 2–48 h. Dose response studies were performed after 12 and 24 h of incubation with IL-1β (0.01–10 ng/ml) or TNF-α (0.1–500 ng/ml), respectively.

2.2. Isolation of total RNA and competitive-quantitative RT-PCR

Total RNA was extracted from cultured cells using the Qiagen RNeasy kit (Valencia, CA). Amplification of AT_1 mRNA was performed using the Titan one tube RT-PCR System (Roche Molecular Biochemicals, Indianapolis, IN). Quantification of AT_1 mRNA levels was done using a quantitative comparative RT-PCR method previously developed by the investigators and is described in detail in Gurantz et al. [22]. Briefly, the DNA fragment of the target AT_1 gene was amplified from three quantities of RNA obtained from the same sample. Determination of RNA concentration was made using two dilutions within the linear range of the spectrophotometric measurement. Amplification was done in the presence of a constant copy number of synthetic deletion mutant cRNA of an AT_{1A} gene clone from which 63 bp were removed (bases 502–564, kindly provided by Dr. Eric Clauser, Collège de France, Paris, France [25]). After separation of the DNA products on an ethidium bromide gel, the intensity of the each band was determined from digitized images. The values for the mutant-derived bands were corrected for the difference in fragment size due to the deletion, and the values for the log target/mutant band intensity were plotted against log RNA concentration. The points were then fitted with a linear line, and the value of x when $y = 0$ was considered the amount of RNA amount that contains the same number of AT_1 mRNA molecules as the mutant cRNA. AT_1 mRNA molecules per nanogram of total RNA was derived from that number. This quantitative comparative RT-PCR method for the estimation of AT_1 mRNA levels was validated by northern analysis in which AT_1 mRNA levels were standardized to either 28s rRNA or GAPDH mRNA as internal standards (unpublished observations from the investigator's laboratory).

2.3. Cloning and packaging of 6 × κB-luciferase

Synthetic oligodeoxynucleotides representing six tandem NF-κB consensus sequences [26] were annealed (forward, 5′-$(GGGACTTTCC)_3$ GAATTC$(GGGACTTTCC)_3$A-3′; reverse, 5′-GATCT$(GGAAAGTCCC)_3$GAATTC$(GGAAAGTCCC)_3$-3′). Annealed oligos were ligated into the *Sma*I-*Bgl*II sites of the luciferase vector, pGL3-Promoter (Promega, Madison, WI) and cloned in *Escherichia coli*. The 6 × κB-luciferase gene was excised from the resulting plasmid by digestion with *Bam*HI-*Sma*I and ligated into the *Not*I sites of the adenoviral shuttle vector, pACCMV.pLpASR [23] using synthetic linker-adapters. A clone that had the luciferase gene inserted in a positive orientation with respect to the adenoviral genome was selected. Adenovirus was produced by recombination between this shuttle vector and the full-length adenovirus 5 vector, pJM17, as described by Gomez-Foix et al. [27].

2.4. Infection of fibroblasts with recombinant adenovirus

Fibroblasts were grown to confluence in 3.5-cm tissue culture plates. Two extra plates were seeded to determine cell number by hemacytometer counting. Fibroblasts were infected with adenovirus (at a multiplicity of infection of 2 plaque forming units per fibroblast) in 1.5 ml DMEM + 2%

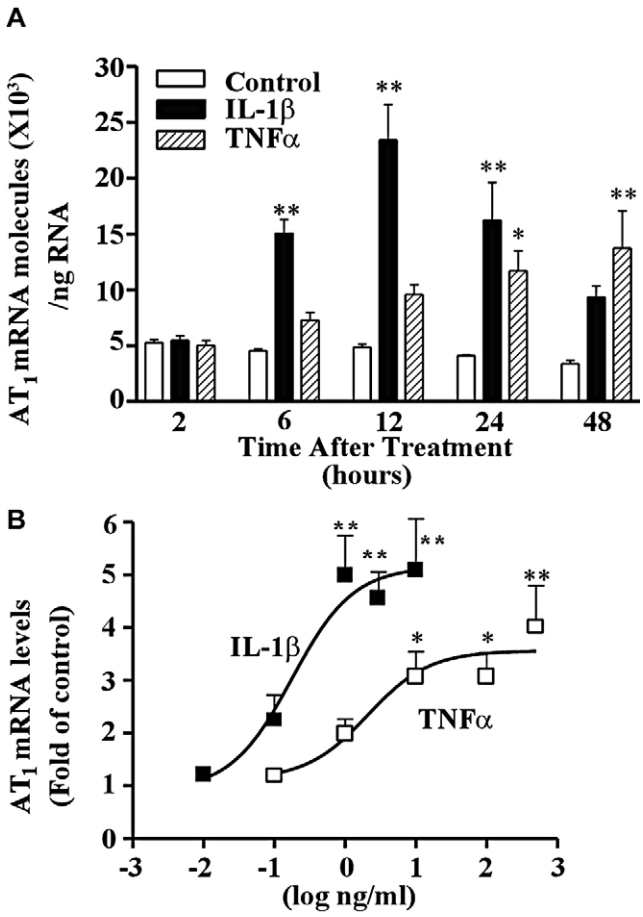

Fig. 1. IL-1β and TNF-α enhance AT_1 mRNA levels in a time and dose-dependent fashion. **A**. Time course: Quantitative RT-PCR determination of AT_1 mRNA molecules per ng total RNA is presented at selected time points after administration of IL-1β (1 ng/ml, black bars) or TNF-α (10 ng/ml, hatched bars). White bars represent AT_1 mRNA content in RNA extracted from untreated (control) fibroblasts. Each value is a mean ± S.E.M. from three independent experiments. **B**. Dose response: Fold increases of AT_1 mRNA levels above control, 12 h after exposure to IL-1β (0.01–10 ng/ml) or 24 h after exposure to TNF-α (0.1–500 ng/ml) are plotted against cytokine concentrations (log ng/ml). Mean ± S.E.M. of three independent experiments is presented. A sigmoid curve fitted to the obtained results yielded an EC_{50} = 0.18 ng/ml (10.5 pM) for IL-1β and 2.1 (123 pM) for TNF-α. $^{*}P < 0.05$, $^{**}P < 0.01$.

fetal bovine serum (heat-inactivated at 65 °C for 15 min) for 18 h. The media was replaced with DMEM + 0.5% fetal bovine serum and the cells were allowed to recover for 6 h. Cells were then treated with cytokine, lysed and assayed for luciferase activity. We had previously found that the efficiency of gene transfer with adenovirus was nearly 100% as indicated by complete inhibition of function by a dominant negative gene that was infected into fibroblasts at multiplicity of infection of 5 plaque forming units per fibroblast (depicted in Fig. 2 in Cowling et al. [23]).

2.5. Luciferase assay

At the desired time-point, cells were washed with PBS and extracted on ice with 200 μl lysis buffer (50 mM Mes/Tris (pH 7.8), 1 mM DTT, 0.1% Triton X-100, 10 μg/ml leupeptin, 0.1 KU/ml aprotinin). Lysates were cleared by centrifugation at 4 °C. Twenty microliters of cell lysate was diluted into 180 μl assay buffer (62.5 mM Mes/Tris (pH 7.8), 12.5 mM $MgCl_2$, 2.1 mg/ml ATP) and loaded into a Monolight 350 Portable Luminescence Photometer (Analytical Luminescence Laboratory Inc., San Diego, CA). The machine was zeroed, 100 μl luciferin solution injected (0.26 mg/ml D(-)-luciferin (Roche) in 5 mM potassium phosphate (pH 7.8) and peak luminescence recorded at room temperature.

2.6. Electrophoretic mobility shift assay (EMSA)

The procedures for preparation of the nuclear extracts from cultured fibroblasts and gel-shift assays for NF-κB were performed as described by Cowling et al. [23].

2.7. Receptor binding assays

Binding of Ang II was performed on intact adherent fibroblasts plated equally in six-well plates. Upon reaching confluence the cells were serum starved and treated with IL-1β, TNF-α or both for 48 h at doses indicated in Section 3 using methods previously described [22]. Non-specific binding was determined in the presence of "cold" Ang II (10^{-5} M), and competition for binding was assessed in the presence of losartan (10^{-5} M Merck, Rahway, NJ) or PD123319 (10^{-5} M RBI, Natick, MA). Based on previous experience in determining the binding characteristics of Ang II to the AT_1 receptor on cardiac fibroblasts [22] a single concentration of 10 nM ^{3}H Ang II was used in these experiments to compare binding levels under different experimental treatments.

2.8. Myocardial infarction and histochemistry

Adult Sprague–Dawley rats were anesthetized by intraperitoneal (IP) administration of a mixture of Ketamine (100 mg/kg) and xylazine (8 mg/kg) and then intubated and placed on a mechanical ventilator. After left thoracotomy was performed, the heart was exposed and the left anterior descending coronary artery was ligated just below its origin. The incision was closed in layers and the rats were allowed to recover. At selected time points from 1 to 83 days post-MI, rats were anaesthetized with the same anesthetic mixture and the heart was excised and cross-sectioned at the center of the scar. The apical part of the heart was frozen for subsequent cryostat sectioning. H and E was used to provide information on scar size and non-myocyte accumulation. Masson staining was used to detect Col.

2.9. Immunohistochemistry

Cytokines were detected using rabbit anti IL-1β (IgG, Serotec, UK) and rabbit anti-rTNF-α polyclonal antibody (IgG, Santa Cruz Biotechnology). AT_1 receptors were detected using rabbit anti-AT_1 polyclonal antibody (IgG, generously provided by Dr. Catt, NIH, Bethesda, MD [28]). Rabbit IgG (Vec-

tor Laboratories, Burlingame CA) was used as negative control. Macrophages were detected using mouse monoclonal antibodies against rat macrophages (Biosource International). Five micrometers cryostat frozen sections of myocardium were fixed by exposure to 4% paraformaldehyde for 20 min and rinsed with PBS for 30 min. Sections were then permeabilized with 0.1% Triton (in 0.1 N sodium citrate) for 5 min at 4 °C and rinsed with PBS for 5 min. PBS was replaced with Tris-buffered saline (TBS) for 10 min. Blocking was performed on tissue sections by using TBS plus 10% blocking serum (of the animal source of the secondary antibody). Incubation with primary antibodies overnight at 4 °C in TBS in the presence of blocking serum was followed by five TBS washes and incubation with secondary antibodies (biotinylated anti-rabbit or anti-mouse IgGs, (Vector Laboratories) in TBS with blocking serum for 60 min at room temperature. Sections were then rinsed five times with TBS and exposed to alkaline-phosphatase streptavidin (in TBS, Vector Laboratories) for 30 min. The chromogen reaction utilized Vector Red as a color substrate (Vector Laboratories). Counter staining with Mayer's hematoxylin for 5 min was used to visualize nuclei and outline of myocytes, similarly to that seen in H and E staining.

2.10. Data analysis

Data are presented as mean ± S.E.M. Significant differences were determined by *t*-test or ANOVA followed by multiple comparison testing using GraphPad Prism software (version 3.00, GraphPad Software, San Diego, CA). A P value <0.05 was considered statistically significant relative to control.

3. Results

3.1. Time- and dose-dependent effects of IL-1β on AT_1 mRNA

Fig. 1A depicts changes in AT_1 mRNA expression (indicated as the number of AT_1 molecules per ng of total RNA) over time in neonatal rat cardiac fibroblasts that were exposed to either IL-1β (1 ng/ml), TNF-α (10 ng/ml) or no treatment. A maximal increase of nearly fivefold in AT_1 mRNA levels occurred 12 h after exposure to IL-1β. This increase in AT_1 mRNA levels was more rapid than was seen with TNF-α. The subsequent decline in AT_1 mRNA levels is likely due to inactivation of IL-1β in the media since the response was sustained at maximal levels over 24 h by re-stimulating with 1 ng/ml IL-1β (data not shown).

Fig. 1B depicts the results of dose response studies performed for IL-1β and TNF-α induced AT_1 mRNA upregulation. IL-1β was about 10-fold more potent than TNF-α as indicated by the EC_{50} values which are 10.5 pM for IL-1β and 123 pM for TNF-α. The maximal effects of IL-1β seen both in the time course and dose response studies were slightly but not significantly greater than those of TNF-α.

3.2. Time course and magnitude of NF-κB activation and nuclear translocation with IL-1β and TNF-α

Since activation of the transcription factor NF-κB is necessary for cytokine induced AT_1 receptor upregulation [23] we tested whether the kinetics of NF-κB activation could account for the time course differences between IL-1β and TNF-α. Fig. 2A depicts a representative time course of luciferase activity from fibroblasts infected with a NF-κB-dependent adenoviral construct and treated with IL-1β or

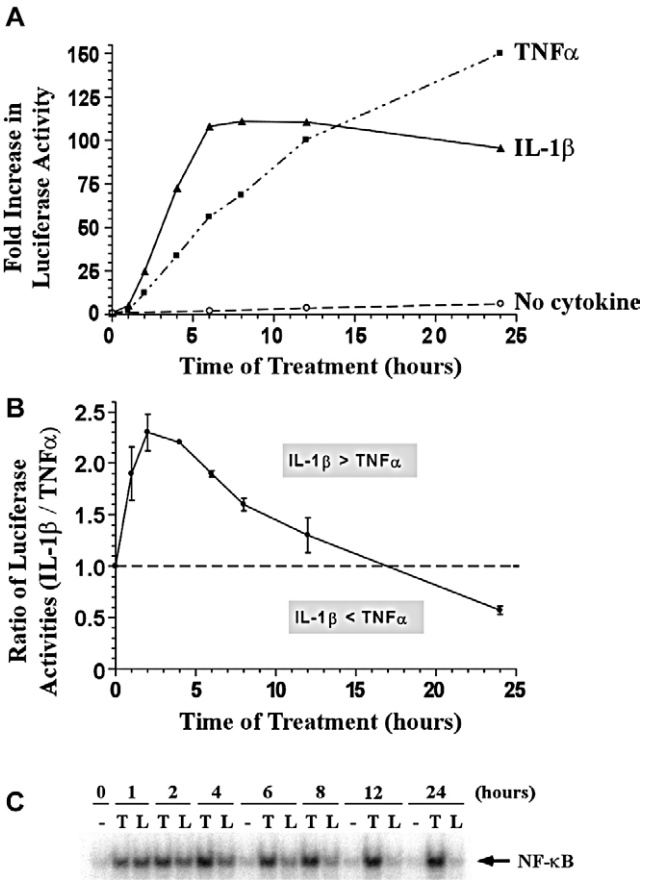

Fig. 2. **A**. TNF-α induces a slower but more sustained activation of a NF-κB-dependent reporter gene than does IL-1β. Confluent fibroblasts that had been infected with 6 × κB-luciferase adenovirus were treated with 5 ng/ml TNF-α (dashed line, closed squares), 0.3 ng/ml IL-1β (solid line, closed triangles) or no cytokine (dashed line, open circles) for the indicated amount of time. Cells were lysed and assayed for luciferase activity as described in Section 2. A representative experiment (of three) depicting fold increase in luciferase activity is shown. **B**. TNF-α-induced reporter activity does not surpass that of IL-1β until after 17 h of treatment. Experiments were performed as described in part A above. The ratio of IL-1β induced luciferase activity to that of TNF-α was plotted versus time of cytokine treatment. Each plotted point represents the mean ± S.E.M. of three independent experiments. A dashed line indicates the position where IL-1β luciferase activity equals that of TNF-α. Above this line IL-1β luciferase activity is greater and below this line TNF-α luciferase activity is greater. **C**. Nuclear translocation of NF-κB is similar at early time points of cytokine administration and is sustained with TNF-α, but not with IL-1β, treatment. Nuclear protein was isolated at time points from fibroblasts treated with IL-1β (0.3 ng/ml, L), or TNF-α (5 ng/ml, T) or no cytokine (–) and used in EMSA to demonstrate binding to the κB consensus sequence. The image of a representative gel (one of three) is depicted.

TNF-α. The increase in luciferase activity with IL-1β was faster and more transient than that with TNF-α, a finding that paralleled cytokine induction of AT_1 mRNA expression (Fig. 1A). A plot of the ratio of luciferase activity induced by IL-1β to that induced by TNF-α consistently showed that the IL-1β effect exceeded that of TNF-α until >17 h of treatment (Fig. 2B). We had previously demonstrated that the prolonged activation of NF-κB nuclear translocation with TNF-α could be explained by low but persistent IKK activity and IκB degradation [23]. EMSA analysis for the level of nuclear NF-κB was performed to determine if nuclear NF-κB levels could explain the differences in rate of activation between the two cytokines. Fig. 2C shows a representative autoradiograph of one of three experiments illustrating the amount of nuclear NF-κB. The nuclear level of NF-κB after IL-1β treatment was similar or less than that of TNF-α at all time points. Thus, at early time points the differences in the rate of gene activation between the two cytokines (seen in Fig. 2A, B) cannot be accounted for by the level of nuclear NF-κB. The reason for this difference between IL-1β and TNF-α is currently not known. However, the subsequent loss of luciferase activity with IL-1β (>6 h, Fig. 2A) seems to be due to the loss of NF-κB from the nucleus (Fig. 2C) since it could be prevented by adding more IL-1β to the cultured fibroblasts (data not shown).

3.3. IL-1β effects on AT_1 mRNA levels and receptor density are additive to those of TNF-α

Since both IL-1β and TNF-α have been detected in the post-MI heart we determined if their effects on AT_1 mRNA expression were additive. In these experiments the effects of combined low, intermediate and high concentrations of IL-1β and TNF-α (as determined from the dose response curves) on AT_1 mRNA expression were evaluated. Combined cytokine stimulation was assessed at 24 h, a time when TNF-α effects on AT_1 mRNA are maximal and significant IL-1β effects are still present. As shown in Fig. 3A, the combination of IL-1β and TNF-α increased AT_1 mRNA levels more than either cytokine alone. At intermediate concentrations the increase in AT_1 mRNA seen with the combination tended to exceed the arithmetic sum of the individual effects (260 ± 41% vs. 168 ± 11%, respectively; $P < 0.08$).

As shown in Fig. 3B intermediate concentrations of individual and combined cytokines increased AT_1 receptor density after 48 h of exposure in a manner similar to that seen with the increase in mRNA levels. The levels of ^{3}H-Ang II (10 nM) specific binding to untreated fibroblasts was 160.3 ± 43 fmol/mg protein. Total specific binding was increased by 80 ± 16% above control by 0.1 ng/ml IL-1β, 130 ± 26% by 1 ng/ml TNF-α and 288 ± 34% by combined treatment (Fig. 3B). Changes in Ang II binding were due to increases in AT_1 receptor density since binding was inhibited by losartan but not by PD123319 (both at 10^{-5} M).

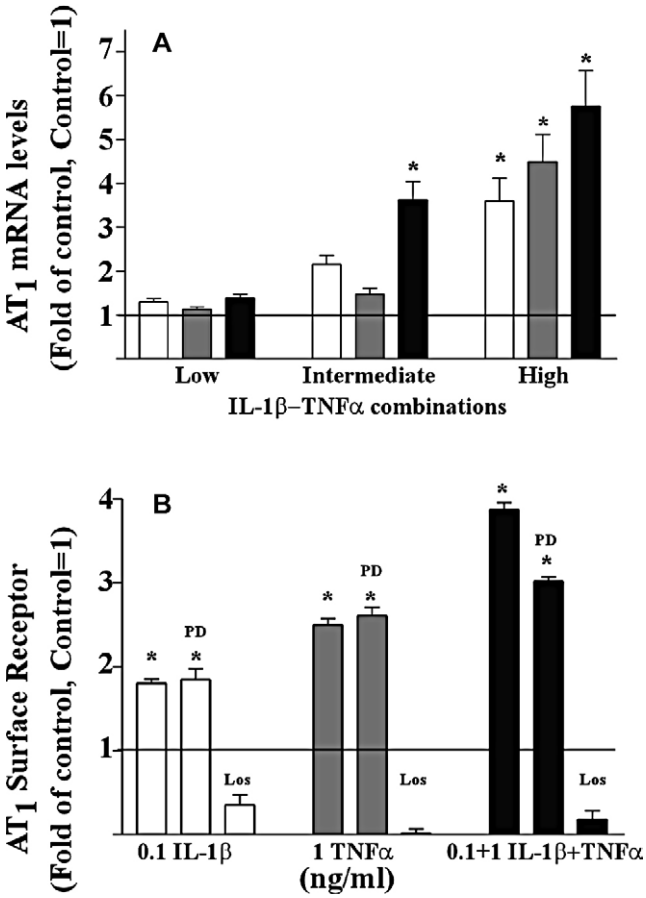

Fig. 3. Submaximal doses of IL-1β and TNF-α combine to enhance AT_1 mRNA levels and AT_1 receptor density. **A**. Fold increases of AT_1 mRNA levels above control 24 h after a single application of IL-1β (open bars), TNF-α (gray bars) or combination (black bars) are plotted for the low, intermediate and high concentration combination pairs, 0.01/0.1, 0.1/1, and 1/10 ng/ml IL-1β and TNF-α, respectively. Data presented as mean ± S.E.M. of three experiments. At intermediate doses the increase in AT_1 mRNA by the combined treatment exceeded the arithmetic sum of increase of either agent alone. *$P < 0.01$ as compared to control. **B**. Fold increases of AT_1 surface receptor density above control, 48 h after a single application of IL-1β at 0.1 ng/ml (open bar), TNF-α at 1 ng/ml (gray bar) or combination (black bar) were determined from binding assays. Data presented as mean ± S.E.M. of three to six experiments (*$P < 0.001$ for difference from control levels). As for mRNA, additivity is observed at the concentration combination of 0.1 and 1.0 ng/ml. Lack of inhibition of binding in the presence of PD123319 and complete inhibition of binding with losatran indicate that the binding is due to the AT_1 receptor subtype.

3.4. Temporal and spatial correlations between appearance of cytokines, increased AT_1 receptor density and deposition of fibrous tissue in the post-MI heart

Previous studies indicate that mRNA and protein concentrations of TNF-α and IL-1β increase in the post-MI heart [18–21]. Since both IL-1β and TNF-α, alone and in combination, increase AT_1 receptor density on cardiac fibroblasts, we assessed the temporal and spatial associations between the appearances of these cytokines and AT_1 receptor density in the post-MI heart. Moreover, since TNF-α induced AT_1 receptor upregulation on cardiac fibroblasts enhances the profibrotic effects of Ang II in cultured cardiac fibroblasts

[24] the relationship between the appearance of the pro-inflammatory cytokines, evidence of increased AT_1 receptor density and the development of fibrosis was also determined.

Fig. 4A, B depict the gross and microscopic changes that occur at representative time points post-MI. As shown in panel A necrotic myocardium in the infarct (I) zone is gradually broken down and replaced by scar tissue as indicated by blue–green color on the Masson stain. This process is essentially complete by 14 days post-MI (data not shown). Microscopic evaluation of the border zone of the infarct (Fig. 4B) shows infiltration of non-myocytes beginning at 1 day post-MI. The accumulation of non-myocytes increases rapidly in this region through day 7 post-MI and, as indicated in column C, includes both macrophages and fibroblasts. Columns B and D demonstrate that the accumulation of cells in the peri-infarction (PI) zone is associated with breakdown of necrotic myocardium in the infarct zone (I) and Col deposition that begins in the PI zone. The extension of non-myocytes and deposition of Col between cardiac myocytes into regions of preserved myocardium outside of the scar is also seen in panel D as early as 3 days post-MI. Although the number of cardiac fibroblasts and macrophages diminishes as the scar is formed (columns B and C), localized accumulations of these cells persist for up to 83 days post-MI at the border between the scar and the non-infarcted myocardium.

Fig. 5 depicts representative examples of microscopic morphology (column A) and immunohistochemical staining for the pro-inflammatory cytokines and the AT_1 receptor (columns B–D, respectively) at the border zone of the infarction at the same post-MI time intervals as in Fig. 4. At day 1 immunostaining for TNF-α, IL-1β and AT_1 receptor is noted in the border zone in association with non-myocytes. The intensity of staining, however, is indistinguishable from that seen in the non-infarcted septum of these rats and from the LV free wall of sham operated rats (data not shown). By day 3 post-MI, non-myocytes accumulate at the PI zone and adjacent myocardium and there is intense immunostaining for TNF-α and IL-1β within these regions (columns B and C). Increased AT_1 receptor immunostaining is also noted in association with both fibroblasts and macrophages, but not with cardiac myocytes. This process reaches its peak between 7 and 14 days post-MI after which the density of non-myocytes and the intensity of immunostaining for TNF-α, IL-1β and the AT_1 receptor gradually diminishes. However, immunostaining for the cytokines and the AT_1 receptor persists in fibroblasts and macrophages at the border between the scar and the non-infarcted myocardium for up to 83 days post-MI.

These results demonstrate the strong temporal and spatial association between the appearance of pro-inflammatory cytokines and increased AT_1 receptor density on non-myocytes in the PI zone. The increases in TNF-α, IL-1β and the AT_1 receptor immunostaining parallel the deposition of fibrous tissue in the infarct zone and surrounding myocardium and they persist in the border zone long after replacement scar formation has been completed. The association between infiltrating fibroblasts and macrophages, immunostaining for TNF-α, IL-1β and the AT_1 receptor is examined in greater detail in Fig. 6 which depicts low, medium and high magnification images of the infarcted LV free wall at 7 days post-MI. At this time point intense staining for both the pro-inflammatory cytokines and for the AT_1 receptor is seen on both cardiac fibroblasts and macrophages. The absence of immunostaining for either the cytokines or AT_1 receptor in association with cardiac myocytes is representative of results obtained at all time points throughout the study.

4. Discussion

Ang II plays an important role in post-MI remodeling of the ECM [2]. Most Ang II effects are mediated through the AT_1 receptor [2,4,5] which is upregulated in the post-MI heart [8,9]. In cultured cardiac fibroblasts TNF-α and IL-1β increase AT_1 receptor density [22], an effect that enhances pro-fibrotic effects of Ang II [24]. Our results demonstrate that IL-1β upregulates the AT_1 receptor more rapidly and at lower concentrations than TNF-α, effects that are mimicked by a NF-κB-dependent luciferase reporter gene. Moreover, the effects of the cytokines in upregulating AT_1 receptor levels are additive. In the post-MI heart strong temporal and spatial associations between the appearance of IL-1β and TNF-α, increases in AT_1 receptor density on non-myocytes and Col deposition in the infarct and PI region were seen. These findings support the concept that, in addition to other recognized effects, IL-1β and TNF-α may also play an important role in the post-MI heart by regulating AT_1 receptor density.

Although both of the pro-inflammatory cytokines studied produce similar maximal increases in AT_1 mRNA and receptor density, IL-1β acts more rapidly and is ~10-fold more potent than TNF-α on a molar basis. Since these cytokines are first seen at about the same time in the PI zone (Fig. 5 [18–21]), IL-1β may provide the initial stimulus for AT_1 increases in this region. Evidence that the effects of the agents are additive suggests that they ultimately act in concert to maintain increased AT_1 density in the post-MI heart and that TNF-α plays an important role in the sustained effect. These findings support the notion of redundancy between cytokines in regulating the AT_1 receptor and they could help explain the lack of efficacy of therapeutic regimens that target only one of these agents [29]. Previous studies indicate that interactions between TNF-α and IL-1β vary depending on the induced effect and cell involved. For example, in rat hepatoma cells TNF-α and IL-1β both individually and together induce acute phase protein genes [30] whereas in cardiac myocytes TNF-α, which alone has no effect on nitric oxide (NO) production, greatly potentiates IL-1β induced NO production through MAP kinase-mediated NF-κB activation [31]. Our results indicate that in cardiac fibroblasts TNF-α and IL-1β converge on the same downstream pathway to increase AT_1 receptor mRNA production.

Our previous work indicated that NF-κB activation was necessary for cytokine induced AT_1 mRNA upregulation in

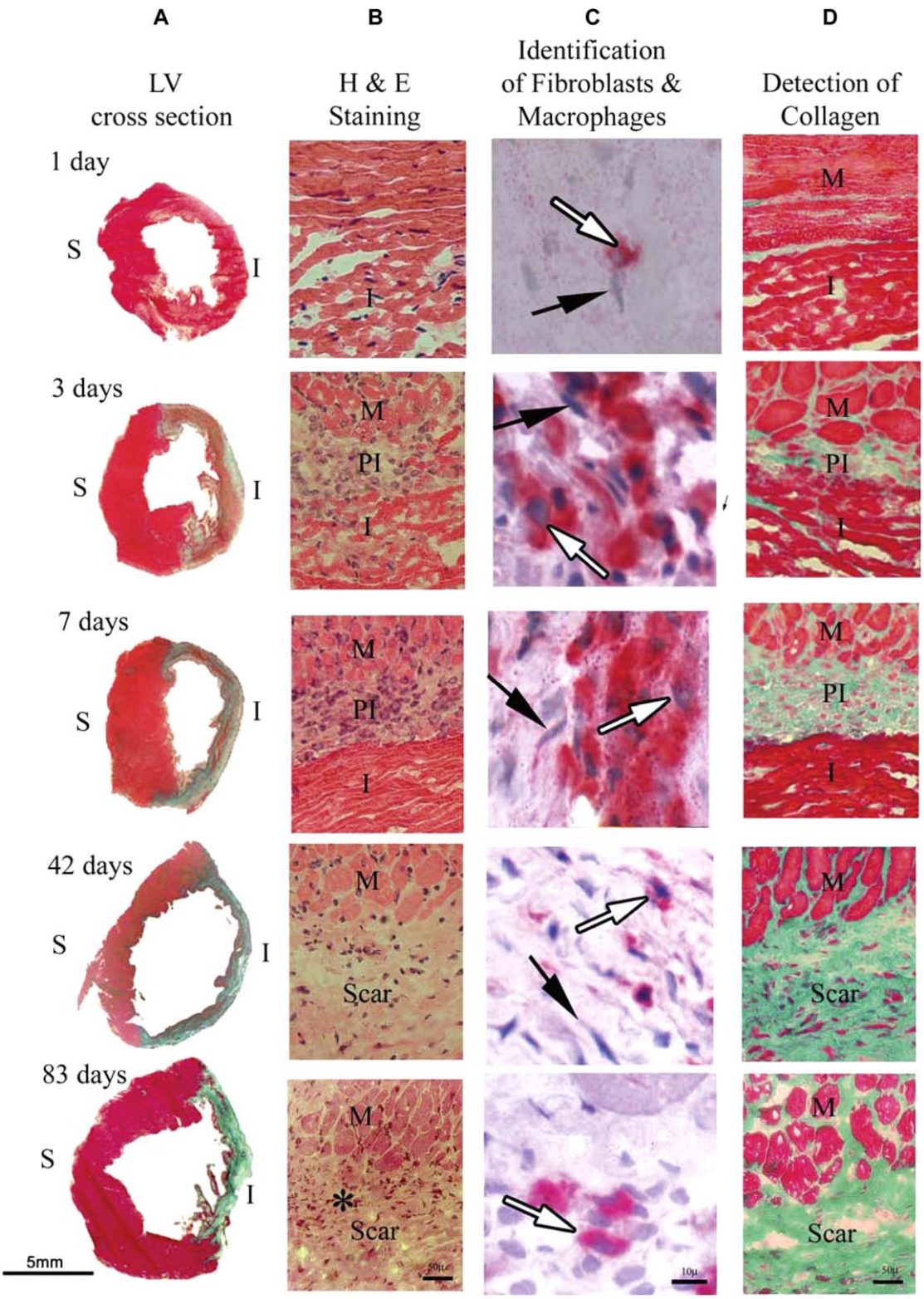

Fig. 4. Evolution of changes in the post-MI left ventricle. The five time-points depicted are representative of the gross and microscopic changes that occur in the LV post-MI. **A**. Cross sections of the LV (with RV removed) stained with Masson trichrome. Necrotic tissue (red) at the infarct zone (I) is gradually replaced with Col (blue green) that forms the scar. **B**. H and E staining shows that by 3 days post-MI non-myocytes cells (dense nuclei stained purple) accumulate between the infarct (I) and the myocytes (M) at the PI zone. Their concentration peaks at 7 days and declines thereafter as scar replacement is completed. *Persistence of non-myocytes at the border is noted as late as 83 days post-MI. **C**. Immunostaining to identify macrophages demonstrates that the mononuclear infiltrate in-between the myocytes consists of macrophages (red stains, white arrow) and fibroblasts (not stained, black arrow). **D**. Amplified trichrome images demonstrate the accumulation of Col at the PI beginning at day 3 and continuing until the necrotic myocardium is replaced by scar tissue. Extension of Col between myocytes bordering the scar is also seen.

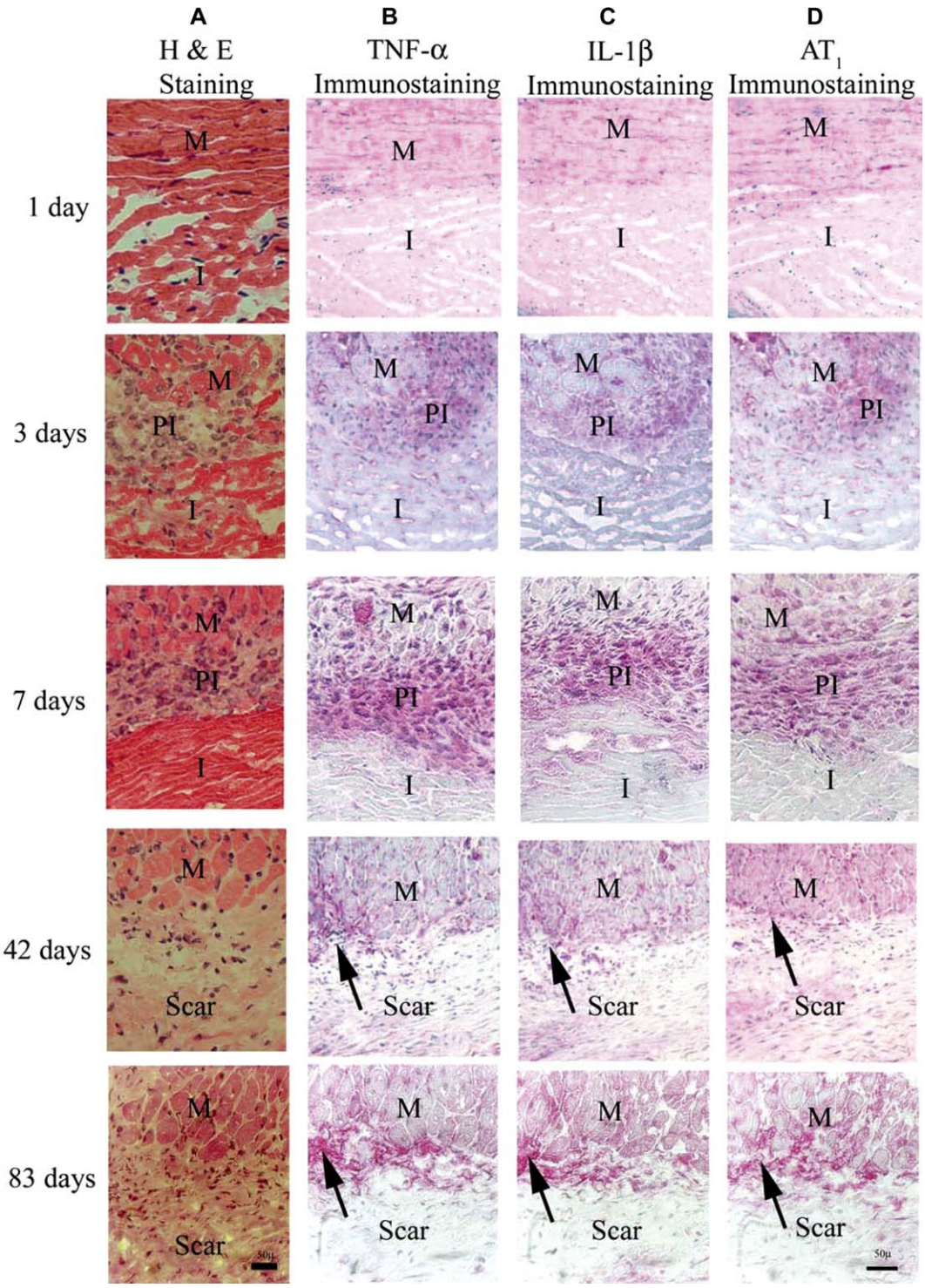

Fig. 5. Appearance of TNF-α, IL-1β and increased AT_1 receptor density at the PI zone. H and E (**A**) and immunostaining for TNF-α (**B**) IL-1β (**C**) and AT_1 (**D**), respectively, are shown for 5 μm serial sections of LV at the times indicated post-MI. At day 3 post-MI increases in the accumulation of the three proteins is observed at the PI zone (red label) with the most intense staining seen at 7 days post-MI. As scar replaces the infarcted myocardium the intensity of the immunostaining for the pro-inflammatory cytokines decreases as does that for the AT_1 receptor. Accumulations of non-myocytes co-localized with immunostaining for cytokines and the AT_1 receptor persist at the border zone for up to 83 days (black arrow). I, infarct region; PI, peri-infarct zone; M, surviving myocytes.

cardiac fibroblasts [23]. The use of NF-κB-dependent reporter constructs demonstrated more rapid activation of NF-κB with IL-1β, a finding that paralleled its effect on AT_1 mRNA. We assessed the possibility that differences between IL-1β and TNF-α induced nuclear translocation of NF-κB might explain the differences in the time course of AT_1 mRNA upregulation with the cytokines. However, as shown in Fig. 2C the initial more rapid increase in transcription with IL-1β is not due to

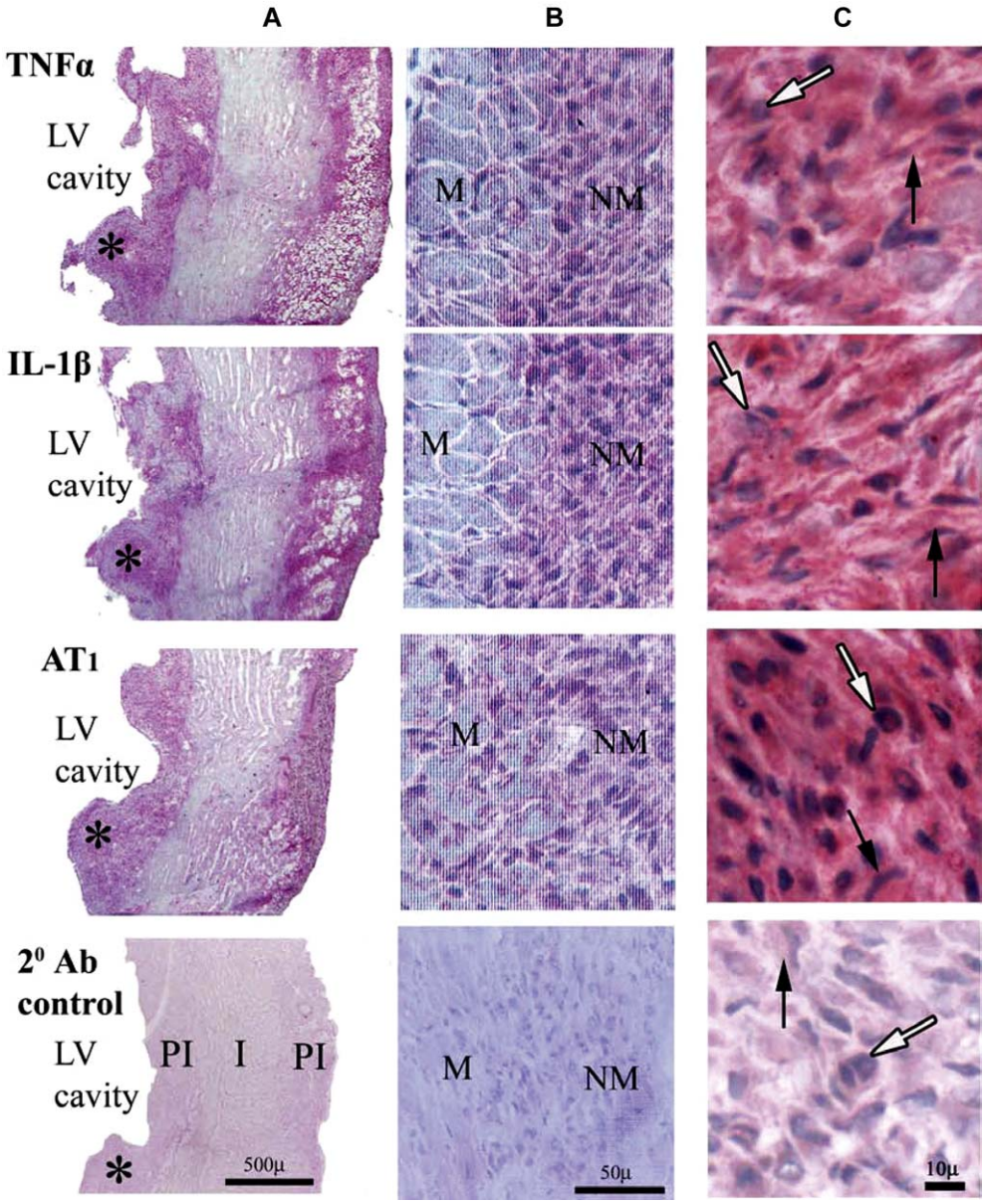

Fig. 6. TNF-α, IL-1β and AT_1 receptor immunostaining is associated with non-myocytes. Immunostaining of the infarct region is shown in three magnifications as indicated by the scale bars. **A**. Accumulation of TNF-α and IL-1β and the high concentration of AT_1 receptor are shown at the border of the infarct along the free wall of the left ventricle. **B**. Labeling of the proteins is associated only with the non-myocytes (*, area magnified from **A**). **C**. Immunostaining is associated with macrophages (white arrow) and fibroblasts (black arrow). Immunostaining using only a secondary antibody results in absence of staining.

increased NF-κB nuclear translocation. Perhaps the NF-κB activated by IL-1β has a greater trans-activation potential than that activated by TNF-α, an effect that could be due to different covalent modifications of NF-κB subunits or associations with ancillary molecules that affect transcriptional competency of NF-κB without affecting the DNA binding determined by EMSA. The EMSA analysis did reveal that the drop in NF-κB-dependent transcription with IL-1β can be explained by loss of NF-κB from the nucleus. As noted in Section 3.2 nuclear NF-κB levels could be maintained by repeated IL-1β administration.

To determine whether the in vitro effects of TNF-α and IL-1β might be involved in regulating AT_1 receptor expression post-MI, we examined the time course for the appearance of these pro-inflammatory cytokines and increased AT_1 receptor density in the post-MI rat heart. Although AT_1 receptor upregulation on non-myocytes in the post-MI rat heart has been noted [8,9], factors involved in this phenotypic change were not evaluated. We noted increased AT_1 receptor density in non-myocytes in the PI zone as early as 2–3 days post-MI that was closely related to appearance of TNF-α and IL-1β immunostaining in this region. Increases in AT_1 receptor density in the PI zone peaked by day 7 post-MI and slowly diminished thereafter. Nonetheless, the presence of these cytokines in association with the AT_1 receptor could still be detected at the border of the replacement scar as late as 83 days post-MI. Throughout the entire time course immunostaining for the AT_1 receptor and the pro-inflammatory cytokines were

closely related. As with the AT_1 receptor, the appearance of the cytokines was associated predominantly with non-myocytes in the PI region. These findings extend previous reports [18–21] by relating the appearance of TNF-α and IL-1β temporally and spatially with increased AT_1 receptor density on non-myocytes in the PI zone and by demonstrating their persistence over an extended period of time post-MI.

The strong association between TNF-α and IL-1β and increased AT_1 receptor density with non-myocytes in the post-MI heart supports the notion that these cytokines induce AT_1 upregulation in an autocrine or paracrine fashion and, thus, may have previously unsuspected effects in regulating the remodeling process. Stimulation of cardiac fibroblasts with Ang II increases production of ECM proteins and the tissue inhibitor of matrix metalloproteinase-1 (TIMP-1). These effects are mediated through the AT_1 receptor. We have shown that in cardiac fibroblasts cytokine induced increases in the AT_1 receptor significantly enhances these effects of Ang II and also reduces MMP-2 production and activity [24]. Thus, the occurrence of cytokine induced AT_1 upregulation in the post-MI heart would favor deposition of fibrous tissue by magnifying the response to Ang II. Early post-MI in the PI zone this effect would benefit the development of the replacement scar. However, increased AT_1 receptor density on non-myocytes also extends into non-infarcted myocardium and in these areas increased fibrosis would adversely affect cardiac function. The persistence of the pro-inflammatory cytokines and increased AT_1 receptor density at the border of the scar for an extended time post-MI has not previously been noted. Although of uncertain significance, it indicates that this border zone remains an active region that potentially could affect cardiac function by further modifying the replacement scar or by producing factors that could influence remodeling in adjacent segments of myocardium.

We found AT_1 receptor immunoreactivity on fibroblasts and macrophages that had accumulated at the PI zone but not on myocytes in any region of the heart. Previous studies indicate the number of AT_1 receptors on cardiac fibroblasts to be in the range of 40,000–100,000 per cell, a number that cytokine induced upregulation is capable of more than doubling [22,32]. The lack of AT_1 immunostaining on cardiac myocytes in the post-MI rat heart is consistent with in vitro observations that rat myocytes in culture express low levels of the AT_1 receptor [4]. These findings support the notion that Ang II effects on myocytes may be related to secretion of 'secondary' growth factors from fibroblasts [6]. Increased AT_1 receptor density in the PI zone involved macrophages as well as fibroblasts. Upregulation of various components of the renin–Ang system including the AT_1 receptor has been observed on monocytes as they migrate from the circulation and differentiate to macrophages in tissue [33]. Our findings indicate that AT_1 receptor density also occurs on macrophages in the PI zone. Although the role of the AT_1 receptor on macrophages in cardiac remodeling has not been extensively studied, AT_1 null mice exhibit reduced macrophage infiltration and cytokine production in the heart post-MI [34] suggesting a role of the AT_1 receptor in mediating Ang II stimulated macrophage chemotaxis and cell migration. Since macrophages are important sources of pro-inflammatory cytokines enhanced migration related to AT_1 receptor upregulation could influence remodeling by increasing cytokine concentrations.

Acknowledgements

The work was supported by funds from a grant (RO1 HL63909; B.H.G.) from the National Institutes of Health. Dr. Randy T. Cowling received support from a post-doctoral fellowship award from the American Heart Association, Western States Affiliate.

References

[1] Beltrami CA, Finato N, Rocco M, Feruglio GA, Puricelli C, Cigola E, et al. Structural basis of end-stage failure in ischemic cardiomyopathy in humans. Circulation 1994;89:151–63.
[2] Weber KT. Extracellular matrix remodeling in heart failure: a role for de novo angiotensin II generation. Circulation 1997;96:4065–82.
[3] Brilla CG, Zhou G, Matsubara L, Weber KT. Collagen metabolism in cultured adult rat cardiac fibroblasts: response to angiotensin II and aldosterone. J Mol Cell Cardiol 1994;26:809–20.
[4] Villarreal FJ, Kim NN, Ungab GD, Printz MP, Dillmann WH. Identification of functional angiotensin II receptors on rat cardiac fibroblasts. Circulation 1993;88:2849–61.
[5] Lijnen PJ, Petrov VV, Fagard RH. Induction of cardiac fibrosis by angiotensin II. Methods Find Exp Clin Pharmacol 2000;22:709–23.
[6] Kim NN, Villarreal FJ, Printz MP, Lee AA, Dillmann WH. Trophic effects of angiotensin II on neonatal rat cardiac myocytes are mediated by cardiac fibroblasts. Am J Physiol 1995;269:E426–E437.
[7] Campbell SE, Katwa LC. Angiotensin II stimulated expression of transforming growth factor-beta1 in cardiac fibroblasts and myofibroblasts. J Mol Cell Cardiol 1997;29:1947–58.
[8] Sun Y, Weber KT. Angiotensin II receptor binding following myocardial infarction in the rat. Cardiovasc Res 1994;28:1623–8.
[9] Lefroy DC, Wharton J, Crake T, Knock GA, Rutherford RA, Suzuki T, et al. Regional changes in angiotensin II receptor density after experimental myocardial infarction. J Mol Cell Cardiol 1996;28:429–40.
[10] Van Krimpen C, Smits JF, Cleutjens JP, Debets JJ, Schoemaker RG, Struyker Boudier HA, et al. DNA synthesis in the non-infarcted cardiac interstitium after left coronary artery ligation in the rat: effects of captopril. J Mol Cell Cardiol 1991;23:1245–53.
[11] De Carvalho FC, Sun Y, Weber KT. Angiotensin II receptor blockade and myocardial fibrosis of the infarcted rat heart. J Lab Clin Med 1997;129:439–46.
[12] Ju H, Zhao S, Jassal DS, Dixon IM. Effect of AT_1 receptor blockade on cardiac collagen remodeling after myocardial infarction. Cardiovasc Res 1997;35:223–32.
[13] Yu CM, Tipoe GL, Wing-Hon LK, Lau CP. Effects of combination of angiotensin-converting enzyme inhibitor and angiotensin receptor antagonist on inflammatory cellular infiltration and myocardial interstitial fibrosis after acute myocardial infarction. J Am Coll Cardiol 2001;38:1207–15.
[14] Taylor K, Patten RD, Smith JJ, Aronovitz MJ, Wight J, Salomon RN, et al. Divergent effects of angiotensin-converting enzyme inhibition and angiotensin II-receptor antagonism on myocardial cellular proliferation and collagen deposition after myocardial infarction in rats. J Cardiovasc Pharmacol 1998;31:654–60.

[15] Dixon IMC, Ju HS, Jassal DS, Peterson DJ. Effect of ramipril and losartan on collagen expression in right and left heart after myocardial infarction. Mol Cell Biochem 1996;165:31–45.

[16] Pfeffer MA, Braunwald E, Moye LA, Basta L, Brown Jr. EJ, Cuddy TE, et al. Effect of captopril on mortality and morbidity in patients with left ventricular dysfunction after myocardial infarction. Results of the survival and ventricular enlargement trial. The SAVE Investigators. N Engl J Med 1992;327:669–77.

[17] Ambrosioni E, Borghi C, Magnani B. The effect of the angiotensin-converting-enzyme inhibitor zofenopril on mortality and morbidity after anterior myocardial infarction. The Survival of Myocardial Infarction Long-Term Evaluation (SMILE) Study Investigators. N Engl J Med 1995;332:80–5.

[18] Herskowitz A, Choi S, Ansari AA, Wesselingh S. Cytokine mrna expression in postischemic/reperfused myocardium. Am J Pathol 1995;146:419–28.

[19] Ono K, Matsumori A, Shioi T, Furukawa Y, Sasayama S. Cytokine gene expression after myocardial infarction in rat hearts: possible implication in left ventricular remodeling. Circulation 1998;98:149–56.

[20] Yue P, Massie BM, Simpson PC, Long CS. Cytokine expression increases in nonmyocytes from rats with postinfarction heart failure. Am J Physiol 1998;275:H250–H258.

[21] Irwin MW, Mak S, Mann DL, Qu R, Penninger JM, Yan A, et al. Tissue expression and immunolocalization of tumor necrosis factor-alpha in postinfarction dysfunctional myocardium. Circulation 1999;99:1492–8.

[22] Gurantz D, Cowling RT, Villarreal FJ, Greenberg BH. Tumor necrosis factor-alpha upregulates angiotensin II type 1 receptors on cardiac fibroblasts. Circ Res 1999;85:272–9.

[23] Cowling RT, Gurantz D, Peng J, Dillmann WH, Greenberg BH. Transcription factor NF-kappa B is necessary for up-regulation of type 1 angiotensin II receptor mrna in rat cardiac fibroblasts treated with tumor necrosis factor-alpha or interleukin-1 beta. J Biol Chem 2002;277:5719–24.

[24] Peng J, Gurantz D, Tran V, Cowling RT, Greenberg BH. Tumor necrosis factor-alpha-induced AT_1 receptor upregulation enhances angiotensin II-mediated cardiac fibroblast responses that favor fibrosis. Circ Res 2002;91:1119–26.

[25] Llorens-Cortes C, Greenberg B, Huang H, Corvol P. Tissular expression and regulation of type 1 angiotensin II receptor subtypes by quantitative reverse transcriptase-polymerase chain reaction analysis. Hypertension 1994;24:538–48.

[26] Lenardo MJ, Baltimore D. NF-Kappa-B—a pleiotropic mediator of inducible and tissue-specific gene-control. Cell 1989;58:227–9.

[27] Gomez-Foix AM, Coats WS, Baque S, Alam T, Gerard RD, Newgard CB. Adenovirus-mediated transfer of the muscle glycogen phosphorylase gene into hepatocytes confers altered regulation of glycogen metabolism. J Biol Chem 1992;267:25129–34.

[28] Smith RD, Baukal AJ, Zolyomi A, Gaborik Z, Hunyady L, Sun L, et al. Agonist-induced phosphorylation of the endogenous AT_1 angiotensin receptor in bovine adrenal glomerulosa cells. Mol Endocrinol 1998;12:634–44.

[29] Mann DL, Mcmurray JJ, Packer M, Swedberg K, Borer JS, Colucci WS, et al. Targeted anticytokine therapy in patients with chronic heart failure: results of the Randomized Etanercept Worldwide Evaluation (RENEWAL). Circulation 2004;109:1594–602.

[30] Baumann H, Morella KK, Wong GH. TNF-alpha, IL-1 beta, and hepatocyte growth factor cooperate in stimulating specific acute phase plasma protein genes in rat hepatoma cells. J Immunol 1993;151:4248–57.

[31] Kan H, Xie Z, Finkel MS. TNF-alpha enhances cardiac myocyte NO production through MAP kinase-mediated NF-kappaB activation. Am J Physiol 1999;277:H1641–H1646.

[32] Gallagher AM, Bahnson TD, Yu H, Kim NN, Printz MP. Species variability in angiotensin receptor expression by cultured cardiac fibroblasts and the infarcted heart. Am J Physiol 1998;274:H801–H809.

[33] Okamura A, Rakugi H, Ohishi M, Yanagitani Y, Takiuchi S, Moriguchi K, et al. Upregulation of rennin–angiotensin system during differentiation of monocytes to macrophages. J Hypertens 1999;17:537–45.

[34] Toko H, Zou Y, Minamino T, Masaya M, Harada M, Nagai T, et al. Angiotensin II type 1a receptor is involved in cell infiltration, cytokine production, and neovascularization in infarcted myocardium. Arterioscler Thromb Vasc Biol 2004;24:664–70.